

## Electronic Supporting Information

### Morphology and electronic structure modulation induced by fluorine doping in nickel-based heterostructures for robust bifunctional electrocatalysis

Pin Hao,<sup>a, †, \*</sup> Wenqian Zhu,<sup>a, †</sup> Fengcai Lei,<sup>a</sup> Xiaoye Ma,<sup>a</sup> Junfeng Xie,<sup>a</sup> Hua Tan,<sup>b</sup> Liyi Li,<sup>c</sup> Hong Liu<sup>b\*</sup> and Bo Tang<sup>a\*</sup>

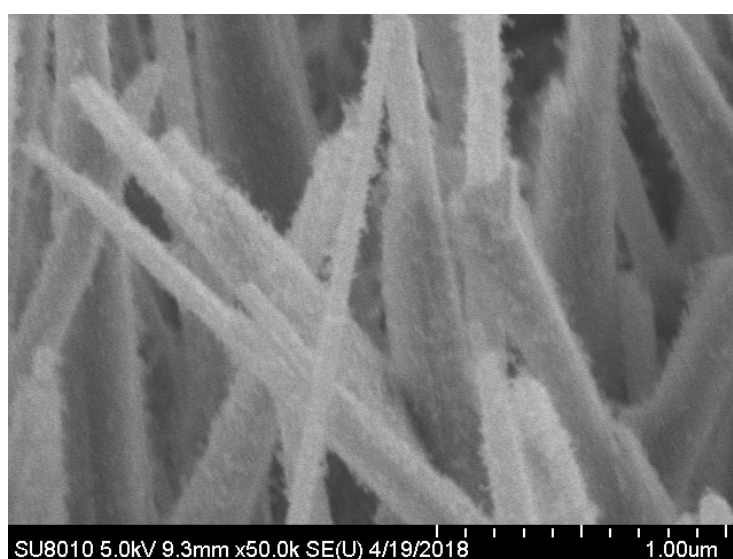


Fig.S1 The magnified SEM image of FN-20

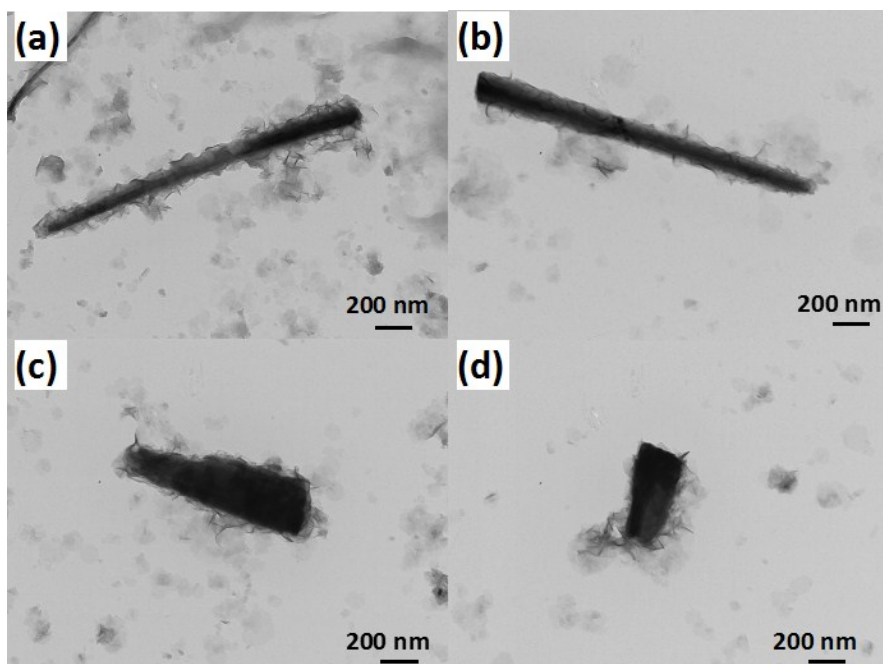


Fig.S2 TEM images of (a) FN-10, (b) FN-15, (c) FN-25 and (d) FN-30

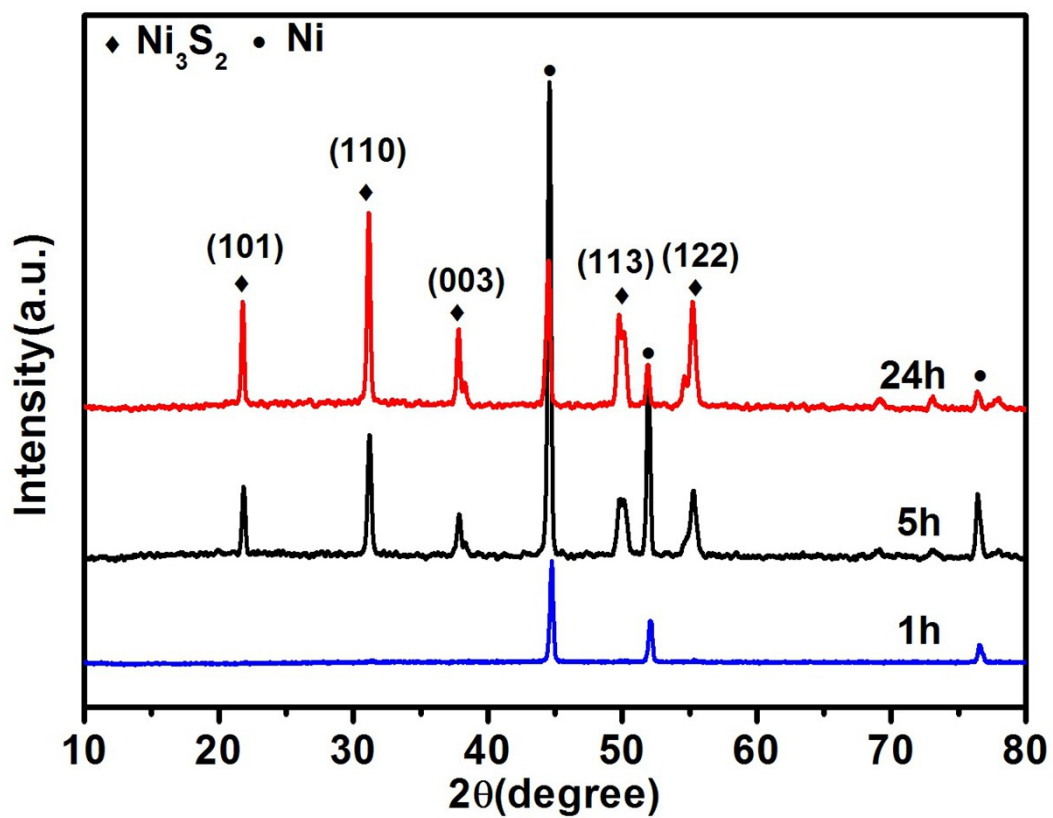


Fig.S3 XRD patterns of samples obtained at different hydrothermal reaction times

Table S1. XPS analysis of the samples at different addition of  $\text{NH}_4\text{F}$ .

XPS analysis (atom%)					
Sample	C	Ni	S	O	F
pristine	32.66	11.73	3.83	51.79	--
FN-10	25.83	20.7	9.47	42.50	1.50
FN-15	27.36	19.63	7.10	44.21	1.70
FN-20	29.27	20.18	7.08	40.95	2.52
FN-25	29.83	20.18	7.02	40.31	2.67
FN-30	27.49	20.36	8.93	40.06	3.16

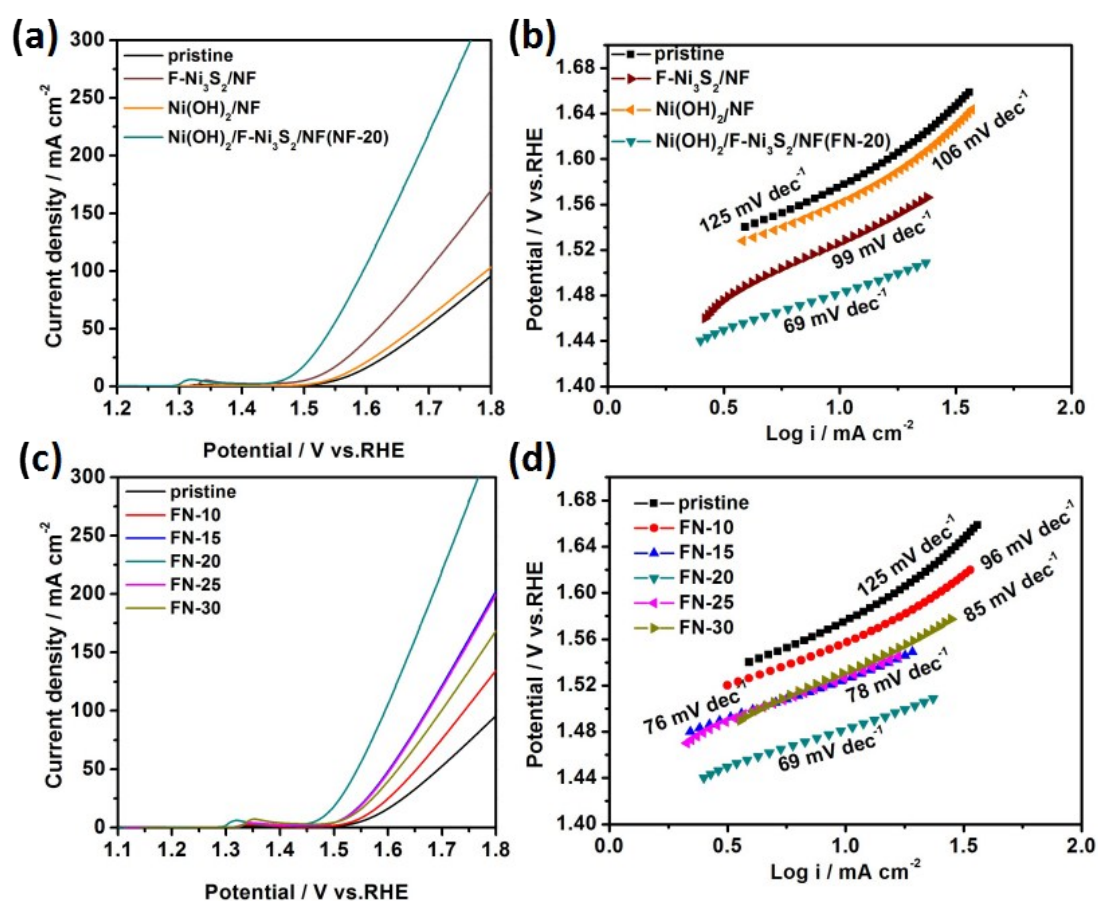


Fig.S4 OER performances in 1 M KOH. (a, b) Linear sweep voltammetry (LSV) curves without IR correction at  $2 \text{ mV s}^{-1}$  and the corresponding Tafel plots of pristine, F-doped  $\text{Ni}_3\text{S}_2$  nanorods,  $\text{Ni}(\text{OH})_2$  nanosheets and FN-20 samples, (c, d) LSV curves without IR correction at  $2 \text{ mV s}^{-1}$  and the corresponding Tafel plots of samples with different addition of  $\text{NH}_4\text{F}$ .

The investigation of the electrochemical surface area (ECSA) of the samples was carried out according to literature.<sup>1</sup> ECSA was estimated by measuring the electrochemical double-

layer capacitance. Cyclic voltammetry (CV) was employed at various scan rates from 20 to 200  $\text{mV s}^{-1}$  in 1.0-1.1 V vs. RHE region, which could be considered as the double-layer capacitive behavior. The electrochemical double-layer capacitance ( $C_{dl}$ ) can be calculated based on the CV curves (Fig.S5a-f). The value of  $C_{dl}$  is estimated by plotting the  $\Delta J$  ( $J_a - J_c$ ) at 1.05 V vs. RHE against the scan rate, where the slope is twice  $C_{dl}$ . The calculated values of double-layer capacitance are as follows: 3.25  $\text{mF cm}^{-2}$ , 3.95  $\text{mF cm}^{-2}$ , 4.0  $\text{mF cm}^{-2}$ , 6.0  $\text{mF cm}^{-2}$ , 5.65  $\text{mF cm}^{-2}$  and 3.8  $\text{mF cm}^{-2}$  for pristine  $\text{Ni}_3\text{S}_2$ , FN-10, FN-15, FN-20, FN-25 and FN-30, respectively. It can be seen that the sample of FN-20 displays a larger  $C_{dl}$  than the other counterparts, indicating that more effective active sites can be exposed for FN-20 and thus contributing to the excellent OER and UOR activity.

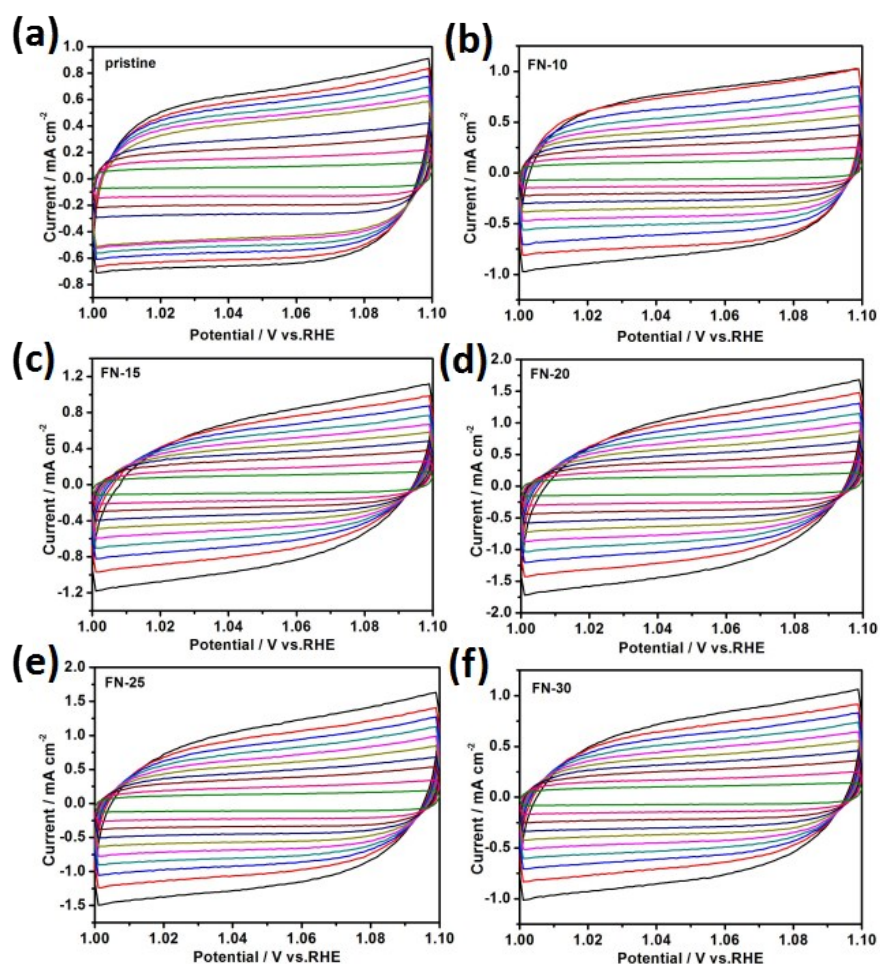


Fig.S5 CV curves of the samples with different  $\text{NH}_4\text{F}$  addition at the various scan rates from 20-200  $\text{mV s}^{-1}$  in non-redox region for the calculation of electrochemical double-layer capacitance.

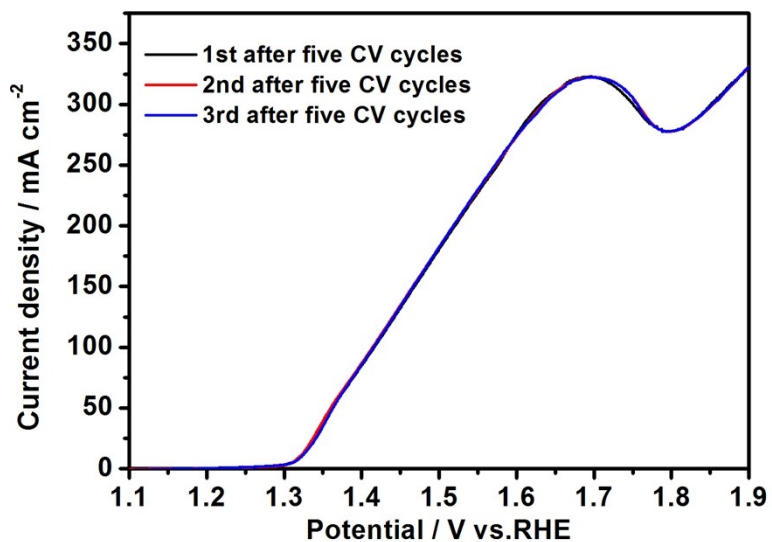


Fig.S6 LSV curves of FN-20 after five CV cycles.

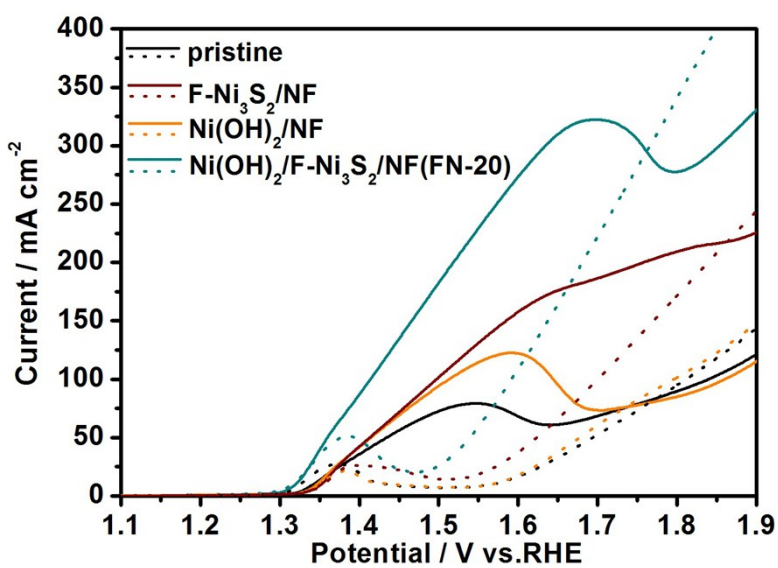


Fig.S7 Comparison of UOR and OER activity of various catalysts, the solid lines and dash lines represent UOR and OER behaviors, respectively.

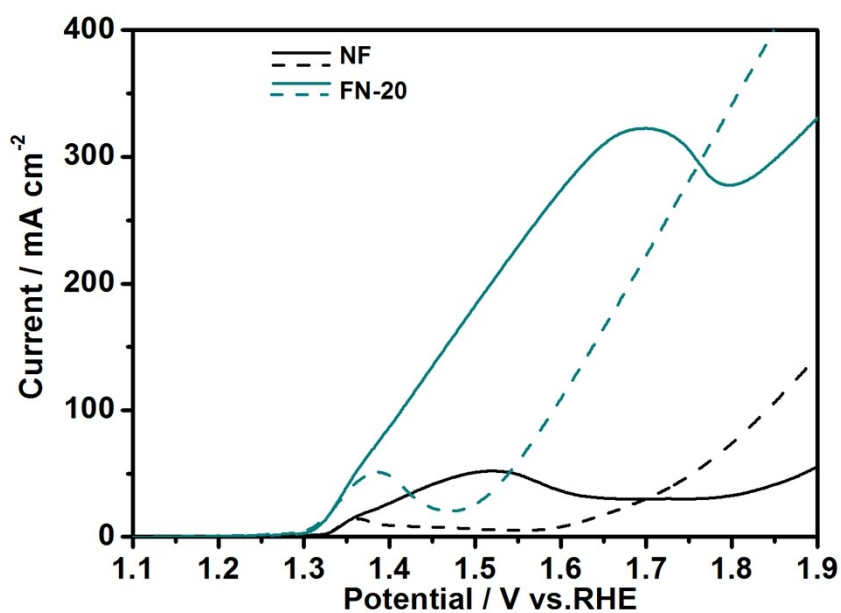


Fig.S8 Comparison of UOR and OER activities of NF and FN-20, the solid lines and dash lines represent UOR and OER behaviors, respectively.

#### Reference

1 J. Xie, J. Zhang, S. Li, F. Grote, X. Zhang, H. Zhang, R. Wang, Y. Lei, B. Pan and Y. Xie, *J. Am. Chem. Soc.*, 2013, **135**, 17881-17888.